Process Optimization with Flexible Pulse Bursts using Bayesian Optimization

Benedikt Bornschlegel[*1], Moritz Kröger[1], Dennis Haasler[2], and Christian Hinke[1]

[1]*RWTH Aachen University - Chair for Laser Technology LLT,*
Steinbachstr. 15, 52074 Aachen, Germany
[2]*Fraunhofer Institute for Laser Technology ILT,*
Steinbachstr. 15, 52074 Aachen, Germany
[*] *Corresponding author's e-mail: benedikt.bornschlegel@llt.rwth-aachen.de*

This study addresses the challenges associated with scaling ablation rates while minimizing surface roughness for copper. By employing tailored flexible bursts, the temporal spacing and energy of individual pulses can be precisely manipulated, creating a high-dimensional parameter space for optimization. Traditional optimization methods are labor-intensive and time-consuming. Thus, we propose an automated Bayesian optimization approach that integrates advanced sensors and a microservice-based software platform for real-time adjustments. Our results demonstrate a multi-objective optimization of removal rates and surface quality, achieving efficiencies of up to 0.16 mm³/minW while reducing surface roughness to as low as 0.33 μm. The findings indicate that effective process optimization by Bayesian optimization is plausible, with the potential for significant advancements in laser processing design. This work underscores the importance of combining Bayesian optimization with expert knowledge to enhance research efficiency and foster further investigations into optimal laser processing conditions.

1. Introduction

The upscaling of ultrashort pulse (USP) laser ablation processes has been a research topic for more than a decade. Throughout the relevant literature multiple approaches for upscaling have been presented and investigated in the past years. Namely there are four main approaches: - scaling by repetition rate, -scaling via multiple beamlets, -scaling by optical stamping and the application of pulse bursts. The application of pulse bursts demonstrates significant potential for the efficient scaling of ablation rate across various materials [1–3]. In addition to the wide variety of materials that can be processed with ultrashort pulses, a key advantage of the burst approach is the low barrier to entry due to the utilization of conventional system technologies, such as galvanometric scanners. Despite the considerable potential exhibited by burst ablation, the small temporal and spatial distances between consecutive pulses amplify shielding effects and heat accumulation, which can lead to detrimental impacts on process quality and efficiency [4]. To control or even leverage these secondary effects, tailored flexible pulse bursts can be employed. These flexible bursts enable the specific manipulation of each pulse within a burst. Consequently, the temporal pulse spacing can be adjusted by completely suppressing pulses or the individual pulse energy can be set to a certain level. By utilizing these flexible bursts, a high-dimensional parameter space becomes available to optimize and tailor bursts to adapt to varying process conditions.

Traditional methods for exploring such high-dimensional parameter spaces are labor-intensive and time-consuming. In contrast, we propose a fully automated Bayesian optimization procedure to streamline material characterization, focusing on maximizing specific removal rates while minimizing surface roughness. Our experimental setup integrates advanced sensors and a microservice-based software platform to facilitate real-time optimization across multiple dimensions. The optimizations produced through this setup are presented and discussed in this work.

2. Setup

The setup used for the fully automated process optimization is shown in Fig. 1. The ultrashort pulse laser beam source FX400 from EdgeWave GmbH has a central wavelength of 1030 nm and a pulse duration of 1.5 ps. The laser beam source allows to vary the amplitude of each pulse within a burst of up to 16 pulses with a pulse spacing of 20 ns. For focusing and deflection of the laser beam an excelliSCAN14 from SCANLAB GmbH with a 160 mm f-theta optic from JENOPTIK AG is utilized and yields a focus diameter $2w_0$ of 33.6 μm. For comparison of the ablation efficiency, cavities with dimensions of 2x2 mm are machined on the sample surface. The scan strategy is a bidirectional line scan with burst overlap BO and line overlap LO of ~ 75 % and rotated by 90° with each layer for a homogenous ablation as schematically shown in Fig. 1b). The burst overlap is hereby defined as the distance between the first pulse of two consecutive bursts, the intraburst pulse distance is neglected. The number of scanned layers n_{rpt} remains constant at 60. The pulse repetition rate f_{rep} is set to 300 kHz and the number of pulses per burst PpB to 6. Therefore, the

remaining parameters for variation are the burst energy. Furthermore, the pulse amplitudes A1 – A6 of the pulses within a burst will be varied.
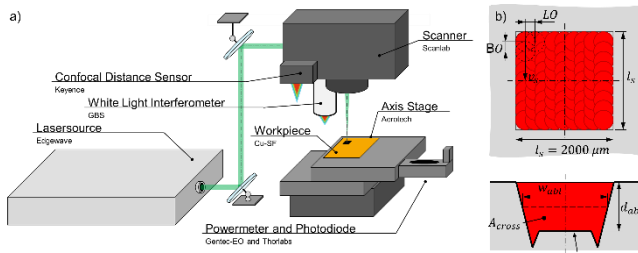

Fig. 1 a) Schematic diagram of the hardware setup used with laser beam source, scanner and axis system, and sensor technology. b) Sketch of the implemented scanning strategy and the measured values for evaluation.

Regarding the analysis capabilities of the system, four sensors are fully integrated. For the depth measurements, necessary for the efficiency evaluation, a confocal distance sensor from KEYENCE AG is used. The surface roughness Sa is determined based on measurements with a white light interferometer (WLI) from GBS metrology GmbH. The laser parameters of the pulse amplitude are measured with a photodiode from Thorlabs GmbH and the average power is determined with a powermeter from Gentec-EO.

As sample material for the validation of the optimization process copper (CW024A) is chosen. Copper ablation with pulse bursts using ultrashort pulse laser radiation has been a topic of research for many years now. Therefore, the occurring effects during ablation like the alternating efficiency with increasing numbers of pluses within a burst [3–5] and, especially, the efficiency increase for 3 PpB [5,6] is well known. This process knowledge provides a good basis for a scientific discussion on the suitability of the process optimization method presented here.

3. Bayesian Optimization

The experiments were designed to optimize both the efficiency ε and surface roughness Sa of the produced cavity. A Multi-Objective Bayesian Optimization (MOBO) approach was utilized to simultaneously optimize these factors. The underlying surrogate model used Gaussian Processes (GP) with Matern 5/2 kernel as a covariance function. As an multi objective acquisition function (responsible for sampling the next parameter set from the surrogate model) qNEHVI [7] was chosen since we expect the inputs to be noisy. The Algorithm was implemented using the Ax and the Botorch Framework [8–11].

Output constraints were set to target efficiencies above 0.02 mm³/minW and surface roughness below 3 μm, effectively defining a region of interest to prevent the algorithm from seeking Pareto-optimal solutions outside this area. The model used individual pulse amplitudes A1 to A6 as input parameters, scalable between 0 and 1. Additionally, a virtual laser power per pulse P_{pulse}, ranging from 0 to 12 W, was introduced to prevent excessive powers that could damage the workpiece by melt based ablation or produce X-rays. Thus, the maximal possible average power within a process is limited to 6 times 12 W, with A1-A6 set to 1. Before running the experiment, the sum of amplitudes A1 to A6 was calculated and multiplied by the selected virtual laser power.

A constraint ensured this sum exceeded 1.0 to protect the laser, as amplitudes below this level would lead to irreparable damage to the amplifier. An overview of the designed algorithm is shown in Fig. 2.
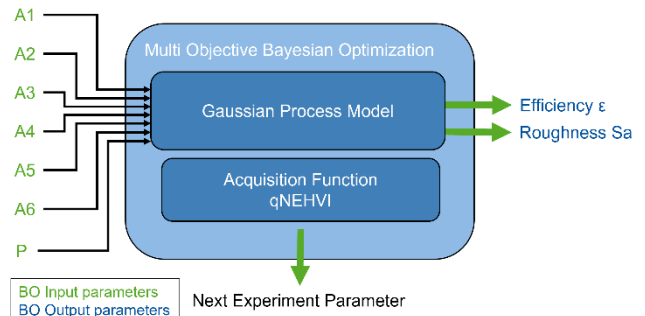

Fig. 2 Overview of the multi objective Bayesian optimization procedure used in this experiment.

A total of 258 trials were conducted, with seven experiments abandoned due to errors in cavity depth measurement. These errors arose when the cavity depth was so small that it could not be reliably detected by the edge detection algorithm. The developed algorithm identifies the edges, reference surface, and bottom surface of the cavity within the measured surface profile. However, when the material removal depth is within the range of surface roughness. In this range, edge detection cannot operate with sufficient accuracy because fine structures and irregularities on the surface significantly hinder the recognition of relevant features. As a result, the actual depth of the ablation cavity cannot be determined. For this reason, these experiments were excluded from consideration and did not contribute to the optimization process. However, this exclusion is not relevant for the application case since the goal is to determine the highest efficiency of the material removal. Therefore, optimization focuses on areas where reliable measurements can be obtained and where significant ablation can be achieved. To prime the Gaussian process model, 14 initial random trials were performed using a Sobol sequence for generation [12].

The execution of the experiment was implemented as follows:

- The underlying Surrogate Model (Sobol or GP) is analyzed with an acquisition function and a new parameter set is generated.
- The parameter set is used to calculate the laser parameters for the experiment
- The parameters are set on the machine and a cavity is produced
- The cavity is analyzed via the WLI and the confocal sensor. The generated data is afterwards feed into an analysis algorithm that determines Sa and the efficiency of the parameter set.
- The results are fed back into the model and the process repeats.

Fig. 3 illustrates hypervolume improvements across trials, with most model improvements occurring in the first 100 trials. The hypervolume is the region spanned between the output constraints for efficiencies and surface roughness and the pareto optimal trials, representing the range of achievable trade-offs. It is therefore bound by the most efficient and least rough solutions within the defined reference space. A larger hypervolume indicates a better overall performance of

the trial set, capturing a more diverse and optimal Pareto front. In Fig. 3, the hypervolume is calculated from experimental data and not the gaussian process model prediction. For more than 100 trials, the hypervolume showed slight improvement, indicating stagnation in the model. Future experiments will explore this further to determine the optimal number of trials needed for a suitable model.
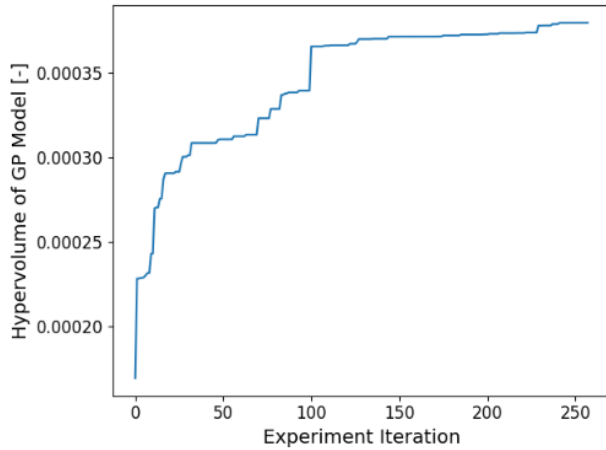

Fig. 3 Course of the hypervolume of the GB model over the number of trials. The apparent saturation of the curve can be seen from iteration 100 onwards.

4. Results

The efficiency of the parameter sets is plotted versus the corresponding surface roughness Sa to build the pareto diagram (Fig. 4). All 258 trials - minus the 7 invalid ones - are shown in Fig. 4. The color coding visualizes the error percentage of the WLI measurements which is the percentage of the missing data points of the gathered 3D point cloud. The explanation for the missing data points is the low reflection on very rough surfaces. As a result, the signal is not sufficient at all lateral points to obtain z information using white light interferometry. Since no error handling was implemented in advance, WLI measurements with a high proportion of missing data points are incorrectly interpreted by the algorithm as a very smooth surface with a low Sa. Which is most likely also the explanation for not measuring higher roughness values than ~2.2 μm. The reason for the missing data points is the measurement technique of the WLI itself, since it is optimized and normally used to measure smooth surfaces with highest precision. However, the optimization algorithm did reach a saturation regime in the hypervolume (Fig. 3), indicating that the optimization may have reached a limit in the output parameters. The incorrectly interpreted data points do affect the convergence speed of the optimization routine since the algorithm tries to find maxima in these areas. This will be automatically detected and removed in future experiments.
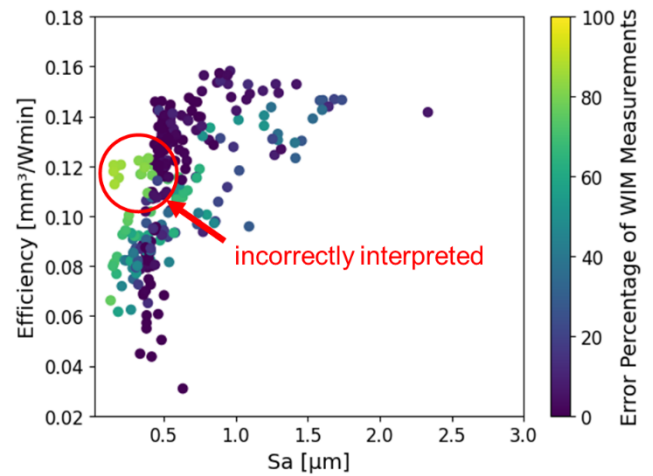

Fig. 4 Pareto diagram of all 258 experiments conducted. The color coding corresponds to the missing data points from the WLI surface measurement. The Pareto front trend is already visible.

To include only reliable measurements in the evaluation, the data was filtered after the optimization for an error percentage of the WLI measurement below 5 %. Thus, reliable data is obtained that can then be filtered an additional time by an algorithm according to the Pareto principle. This results in a pareto front consisting of 14 unique data sets shown in Fig. 5 and Table 1. It becomes evident that there is a limitation of the accessible efficiency of the ablation process around 0.16 mm³/minW. The theoretical background of this limitation lays within the laser-material-interaction itself. Due to the chosen constraints the algorithm stays in the ultrashort pulsed ablation regime without melt ejection by heat accumulation. Therefore, the material gets ablated by evaporation, sublimation, spallation and phase explosion. This process can be described by a threshold model [13] where material is ablated if a fluence above that threshold is applied. Based on that model an efficiency model with a maximum ε_{max} at e^2 times of the threshold fluence F_{th} can be derived [14,15]. This maximum depends on material properties and laser specifications. In this case the 0.16 mm³/minW are in good agreement with literature values for copper ablation by ultrashort pulses [2,4,16].

However, the potential is shown to decrease the surface roughness *Sa* after machining to 0.44 μm by only losing 0.01 mm³/minW in efficiency. A further decrease of the Sa value down to 0.33 μm can be realized, but the efficiency drops down to 0.08 mm³/minW in this case. Which corresponds to 50 % of the highest efficiency reached in these trials.
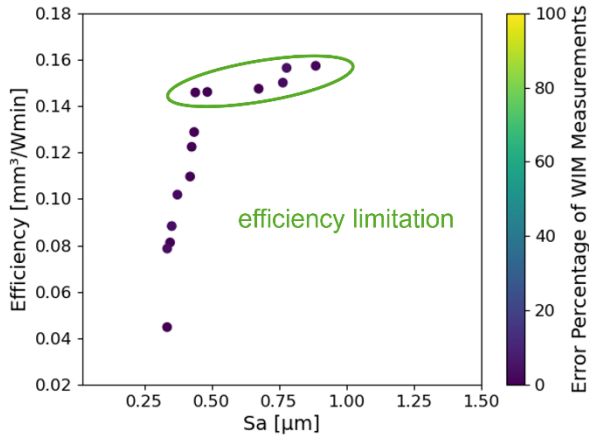
Fig. 5 Pareto diagram with 14 data sets after filtering for <5% missing surface data and filtering according to the Pareto principle. The Pareto front is clearly visible and shows a limitation at ε = 0.16 mm³/minW and Sa = 0.33 µm.

Table 1 displays the corresponding iteration number, the single pulse peak fluences of the six burst pulses and the resulting surface roughness Sa and efficiency ε. The group of data sets reaching the limitation of efficiency as marked in Fig. 5 are also marked green in Table 1. It becomes evident that for these data sets the single pulse peak fluences for many pulses lies within the known optimum range for single pulse copper ablation of around $F_{max} = 5$ J/cm² where ε_{max} is reached[2,4,5]. For the less efficient parameter sets on the Pareto front, all pulses except one show a single pulse peak fluence that is below the optimal fluence. This is therefore consistent with the model presented in the literature for the efficiency of ultra-short pulsed ablation and the experimental data for copper burst processing and therefore suggests that the optimization of the process via MOBO is plausible.

Table 1 The data sets corresponding to the Pareto front showing the single pulse peak fluences, the efficiency and the surface roughness. The sets reaching the efficiency limitation are marked in green.

Dataset	Iteration	F1 [J/cm²]	F2 [J/cm²]	F3 [J/cm²]	F4 [J/cm²]	F5 [J/cm²]	F6 [J/cm²]	Sa [µm]	ε [mm³/minW]
0	32	2,22	1,17	5,83	0	0	0,47	0,43	0,13
1	42	1,62	0	3,87	0	0,35	1,01	0,35	0,08
2	60	3,17	1,42	2,25	0	0	4,17	0,35	0,09
3	79	0	0,94	3,13	1,19	0,75	2,63	0,42	0,11
4	118	2,01	1,97	0	2,24	0,57	3,79	0,43	0,12
5	127	2,49	0,44	0	2,29	1,08	4,02	0,48	0,15
6	139	0,49	1,73	1,81	0,36	0,7	0,52	0,33	0,04
7	144	5,03	0	1,34	6,37	5,35	5,86	0,78	0,16
8	150	0	2,53	0	4,02	2,09	2,17	0,33	0,08
9	172	5,39	0	1,11	6,92	5,74	6,78	0,76	0,15
10	198	0	0	5,16	4,52	6,37	0	0,67	0,15
11	207	1,88	0,64	0	2,37	0,79	3,76	0,44	0,15
12	208	2,85	0,61	0	3,24	0,48	4,38	0,37	0,10
13	217	3,13	0	1,2	5,45	4,39	6,65	0,89	0,16

For better comparability of the burst shape, the relative pulse amplitudes normalized to the highest fluence within a burst are shown in Fig. 6. For five of the six parameter sets a variation of a pre-pulse followed by two pulses with 0 J/cm² or close to it and a triple pulse burst can be seen. For trial number 198, the algorithm only suggests a triple pulse with 3 pulses, whereby the other pulses are completely suppressed. These, by the Bayesian optimization created constellations for high efficiency are also very plausible

compared to literature. For triple pulse burst (3 PpB) with pulse spacings in the regime of 20 ns as used in this experiment, an efficiency increase up to 20 % is reported [5,6]. It is also reported that the second pulse within a burst is most likely the cause of redeposition or strong shielding effects [4,17,18], which hinders the efficient ablation of material. Thus, the suppression of these pulses by the algorithm correlates with reaching high efficiency and makes the results plausible.
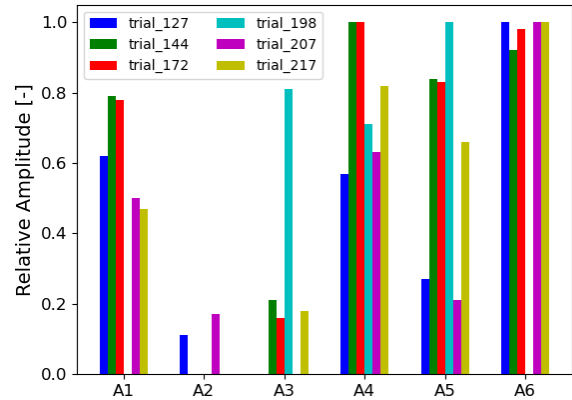

Fig. 6 The relative pulse amplitudes of the six parameter sets reaching the efficiency limitation marked in Fig. 5.

5. Conclusion

The application of Multi-Objective Bayesian Optimization (MOBO) in process development, particularly in the context of USP laser processing, demonstrates promising potential for rapid data generation in complex, multidimensional problems. Despite the efficiency of MOBO, specialized knowledge remains essential for experiment design. The planning and execution of experiments must be guided by experts to effectively identify and control relevant parameters. A significant limitation in the application of MOBO is the restriction on input parameters, such as the 12 W constraint in this example. This limitation can hinder optimization flexibility and must be carefully considered.

A detailed understanding of the sensors used is necessary to ensure accurate measurements. In this case, a misinterpretation regarding surface roughness occurred, which needs to be addressed. MOBO serves as a valuable tool for quickly identifying promising process windows that warrant further investigation. This capability can significantly enhance research efficiency. However, it is crucial to emphasize that MOBO will not replace scientific research. Instead, it acts as a supportive tool by suggesting interesting process windows for more detailed investigations. Without specialized process knowledge, no relevant process understanding can be generated.

Furthermore, additional investigations are needed to validate the results obtained through MOBO and to conduct physical interpretations. These steps are essential to fully leverage the capabilities of MOBO methods and to translate the findings into practical applications. Overall, the combination of MOBO with solid expertise and further research efforts can propel the development of more efficient processes in the USP laser material processing domain.

References
[1] N. Hodgson, H. Allegre, A. Starodoumov, and S. Bettencourt: J. Laser Micro Nanoeng., 15, (2020) 236.
[2] B. Jäggi, L. Cangueiro, D. Bruneel, J. A. Ramos de Campos, C. Hairaye, and B. Neuenschwander: Proc. SPIE, Vol. 10519, (2018) 1051905.
[3] D. J. Förster, B. Jäggi, A. Michalowski, and B. Neuenschwander: Materials, 14, (2021) 3331.
[4] B. Bornschlegel and J. Finger: J. Laser Micro Nanoeng., 14, (2019) 88.
[5] A. Žemaitis, P. Gečys, M. Barkauskas, G. Račiukaitis, and M. Gedvilas: Sci. reports, 9, (2019) 12280.
[6] T. Kramer, B. Neuenschwander, B. Jäggi, S. Remund, U. Hunziker, and J. Zürcher: Phys. Procedia, 83, (2016) 123.
[7] S. Daulton, M. Balandat, and E. Bakshy: arXiv, (2021) 2105.08195.
[8] pytorch: BoTorch, online available at: <https://github.com/pytorch/botorch> (Accessed 9 July 2025).
[9] facebook: Ax, online available at: <https://github.com/facebook/Ax> (Accessed 9 July 2025).
[10] M. Balandat, B. Karrer, D. R. Jiang, S. Daulton, B. Letham, A. G. Wilson, and E. Bakshy: arXiv, (2019) 1910.06403.
[11] M. Olson, E. Santorella, L. C. Tiao, S. Cakmak, D. Eriksson, M. Garrard, S. Daulton, M. Balandat, E. Bakshy, E. Kashtelyan, Z. J. Lin, S. Ament, B. Beckerman, E. Onofrey, P. Igusti, C. Lara, B. Letham, C. Cardoso, S. S. Shen, A. C. Lin, and M. Grange: AutoML 2025 ABCD Track, (2025).
[12] I. Sobol': USSR Computational Mathematics and Mathematical Physics, 7, (1967) 86.
[13] S. Nolte, C. Momma, H. Jacobs, A. Tünnermann, B. N. Chichkov, B. Wellegehausen, and H. Welling: J. Opt. Soc. Am. B, 14, (1997) 2716.
[14] G. Raciukaitis: J. Laser Micro Nanoeng., 4, (2009) 186.
[15] B. Neuenschwander, G. F. Bucher, C. Nussbaum, B. Joss, M. Muralt, U. W. Hunziker, and P. Schuetz: Proc. SPIE, Vol. 7584, (2010) 75840R.
[16] B. Neuenschwander, T. Kramer, B. Lauer, and B. Jaeggi: Proc. SPIE, Vol. 9350, (2015) 93500U.
[17] D. J. Förster, S. Faas, S. Gröninger, F. Bauer, A. Michalowski, R. Weber, and T. Graf: Appl. Surf. Sci., 440, (2018) 926.
[18] B. Bornschlegel, M. Kratz, and J. Finger: J. Laser Micro Nanoeng., 17, (2022) 19.